JOC*Note*

Structure, Stereodynamics and Absolute Configuration of the Atropisomers of Hindered Arylanthraquinones

Lodovico Lunazzi, Michele Mancinelli,† and Andrea Mazzanti*

Department of Organic Chemistry "A. Mangini", University of Bologna, Viale Risorgimento 4, Bologna 40136, Italy

mazzand@ms.fci.unibo.it

Received October 24, 2008

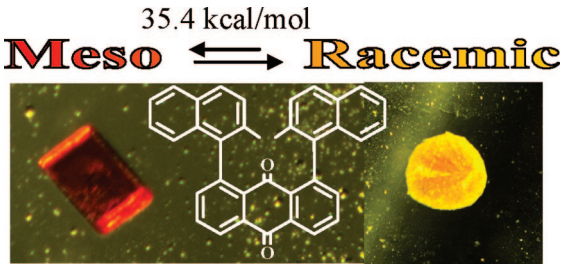

Anthraquinone substituted by 2-methyl-1-naphthyl groups in positions 1,8 yields *syn* (meso) and *anti* (racemic) isomers (red and yellow colored, respectively) that interconvert with a barrier of 35.4 kcal mol^{-1} in solution. Their structures were identified by NOE experiments in solution and X-ray diffraction in the solids. The racemic *anti* form (C_2 point group) entails two atropisomers that were separated by enantioselective HPLC: the absolute configuration was assigned by TD-DFT simulation of the ECD spectrum. Two atropisomers were also separated and assigned in the case of anthraquinone bearing a single 2-methyl-1-naphthyl substituent in position 1.

Atropisomers arising from restricted sp^2-sp^2 rotation of two aryl substituents bonded to appropriate positions of planar (or *quasi* planar) frameworks have been reported.[1−8] In the majority of cases, the atropisomers arising from this rotation process were identified by spectroscopic methods since quite often the lifetimes of these species were not sufficiently long-lived to allow a physical separation to be achieved. In particular, configurationally stable atropisomers containing the anthraquinone moiety have not been reported, to the best of our knowledge. Configurationally stable atropisomers with the anthraquinone skeleton are quite interesting since this moiety can be easily functionalized, so we synthesized an anthraquinone derivative bearing 2-methyl-1-naphtyl substituents in the 1,8 positions (compound **1** of Chart 1).

CHART 1

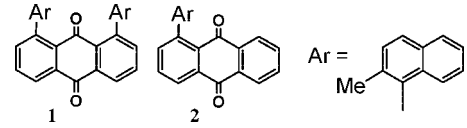

SCHEME 1

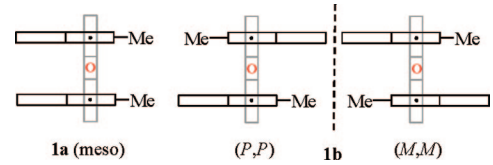

Compound **1** exists as the *syn* isomer (**1a**), which is a meso form (C_s point group), and the *anti* isomer (**1b**), which is racemic (C_2 point group), as shown in Scheme 1.

According to DFT calculations,[9] the barrier[10] for the *anti* (**1b**) to *syn* (**1a**) interconversion is expected to be as high as 33.5

† In partial fulfillment of the requirements for a Ph.D. degree in Chemical Sciences, University of Bologna.

(1) Mitchell, R. H.; Yan, J. S. H. *Can. J. Chem.* **1980**, *58*, 2584–2587. Dell'Erba, C.; Gasparrini, F.; Grilli, S.; Lunazzi, L.; Mazzanti, A.; Novi, M.; Pierini, M.; Tavani, C.; Villani, C *J. Org. Chem.* **2002**, *67*, 1663–1668. Chen, C.-T.; Chadha, R.; Siegel, J. S.; Hardcastle, H. *Tetrahedron Lett.* **1995**, *36*, 8403–8406. Lunazzi, L.; Mazzanti, A.; Minzoni, M.; Anderson, J. E. *Org. Lett.* **2005**, *7*, 1291–1294. Mazzanti, A.; Lunazzi, L.; Minzoni, M.; Anderson, J. E. *J. Org. Chem.* **2006**, *71*, 5474–5481.

(2) (a) Clough, R. L.; Roberts, J. D. *J. Am. Chem. Soc.* **1976**, *98*, 1018–1020. (b) Cozzi, F.; Cinquini, M.; Annunziata, R.; Siegel, J. S. *J. Am. Chem. Soc.* **1993**, *115*, 5330–5331. (c) Cozzi, F.; Ponzini, F.; Annunziata, R.; Cinquini, M.; Siegel, J. S. *Angew. Chem., Int. Ed. Engl.* **1995**, *34*, 1019–1020. (d) Zoltewicz, J. A.; Maier, N. M.; Fabian, W. M.F. *Tetrahedron* **1996**, *52*, 8703–8706. (e) Zoltewicz, J. A.; Maier, N. M.; Fabian, W. M. F. *J. Org. Chem.* **1996**, *61*, 7018–7021. (f) Thirsk, C.; Hawkes, G. E.; Kroemer, R. T.; Liedl, K. R.; Loerting, T.; Nasser, R.; Pritchard, R. G.; Steele, M.; Warren, J. E.; Whiting, A. *J. Chem. Soc., Perkin Trans. 2* **2002**, 1510–1519. (g) Tumambac, G. E.; Wolf, C. *J. Org. Chem.* **2005**, *70*, 2930–2938.

(3) Lai, J.-H. *J. Chem. Soc., Perkin Trans. 2* **1986**, 1667–1670.

(4) (a) House, H.; Hrabie, J. A.; Van Derveer, D. *J. Org. Chem.* **1986**, *51*, 920–929. (b) House, H.; Holt, J. T.; Van Derveer, D. *J. Org. Chem.* **1993**, *58*, 7516–7523. (c) Lunazzi, L.; Mancinelli, M.; Mazzanti, A. *J. Org. Chem.* **2007**, *52*, 5391–5394.

(5) Cross, W.; Hawkes, G. E.; Kroemer, R. T.; Liedl, K. R.; Loerting, T.; Nasser, R.; Pritchard, R. G.; Steele, M.; Watkinson, M.; Whiting, A. *J. Chem. Soc., Perkin Trans. 2* **2001**, 459–467.

(6) Lai, Y.-H.; Chen, P. *J. Chem. Soc., Perkin Trans. 2* **1989**, 1665–1670.

(7) Cozzi, F.; Annunziata, R.; Benaglia, M.; Baldrige, K. K.; Aguirre, G.; Estrada, J.; Sritana-Anant, Y.; Siegel, J. S. *Phys. Chem. Chem. Phys.* **2008**, *10*, 2686–2694.

(8) Lunazzi, L.; Mancinelli, M.; Mazzanti, A. *J. Org. Chem.* **2008**, *73*, 5354–5359.

(9) Frisch, M. J.; Trucks, G. W.; Schlegel, H. B.; Scuseria, G. E.; Robb, M. A.; Cheeseman, J. R.; Montgomery, J. A., Jr.; Vreven, T.; Kudin, K. N.; Burant, J. C.; Millam, J. M.; Iyengar, S. S.; Tomasi, J.; Barone, V.; Mennucci, B.; Cossi, M.; Scalmani, G.; Rega, N.; Petersson, G. A.; Nakatsuji, H.; Hada, M.; Ehara, M.; Toyota, K.; Fukuda, R.; Hasegawa, J.; Ishida, M.; Nakajima, T.; Honda, Y.; Kitao, O.; Nakai, H.; Klene, M.; Li, X.; Knox, J. E.; Hratchian, H. P.; Cross, J. B.; Bakken, V.; Adamo, C.; Jaramillo, J.; Gomperts, R.; Stratmann, R. E.; Yazyev, O.; Austin, A. J.; Cammi, R.; Pomelli, C.; Ochterski, J. W.; Ayala, P. Y.; Morokuma, K.; Voth, G. A.; Salvador, P.; Dannenberg, J. J.; Zakrzewski, V. G.; Dapprich, S.; Daniels, A. D.; Strain, M. C.; Farkas, O.; Malick, D. K.; Rabuck, A. D.; Raghavachari, K.; Foresman, J. B.; Ortiz, J. V.; Cui, Q.; Baboul, A. G.; Clifford, S.; Cioslowski, J.; Stefanov, B. B.; Liu, G.; Liashenko, A.; Piskorz, P.; Komaromi, I.; Martin, R. L.; Fox, D. J.; Keith, T.; Al-Laham, M. A.; Peng, C. Y.; Nanayakkara, A.; Challacombe, M.; Gill, P. M. W.; Johnson, B.; Chen, W.; Wong, M. W.; Gonzalez, C.; Pople, J. A. *Gaussian 03*, Revision E.01; Gaussian, Inc., Wallingford, CT, 2004.

(10) Computations indicate the *anti* conformer to be 0.35 kcal mol^{-1} more stable than the *syn* conformer. In the transition state required to accomplish their interconversion, the methyl group of one naphthalene ring crosses over the C=O moiety. The alternative transition state, where the methyl group crosses over position 2 of anthraquinone, has a higher computed energy (37.7 kcal mol^{-1}) so that the corresponding pathway is not expected to take place.

10.1021/jo802383s CCC: $40.75 © 2009 American Chemical Society
Published on Web 12/23/2008

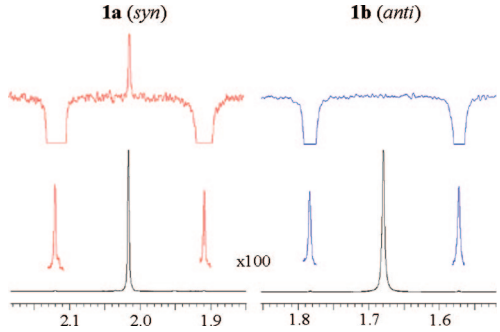

FIGURE 1. (Left) ^{1}H methyl signal of **1a** (600 MHz in $CDCl_3$) with the 100-fold amplified ^{13}C satellites in the inset of the lower trace. The NOE effect, obtained by irradiating these satellites, is shown in the top trace (red). (Right) Methyl signal of **1b** with the amplified ^{13}C satellites. The same experiment does not yield any NOE effect here (top trace, blue).

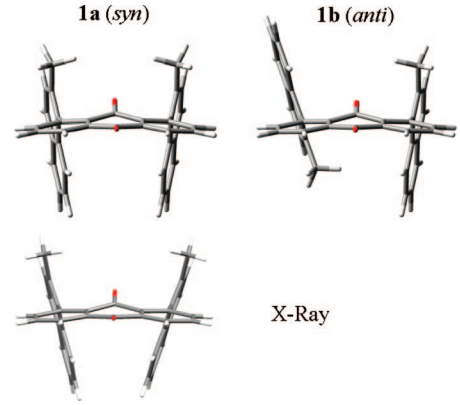

FIGURE 2. (Top) DFT-computed ground state of the *syn* (**1a**) and *anti* (**1b**) isomers of **1**. Underneath is the X-ray structure determined for **1a**.

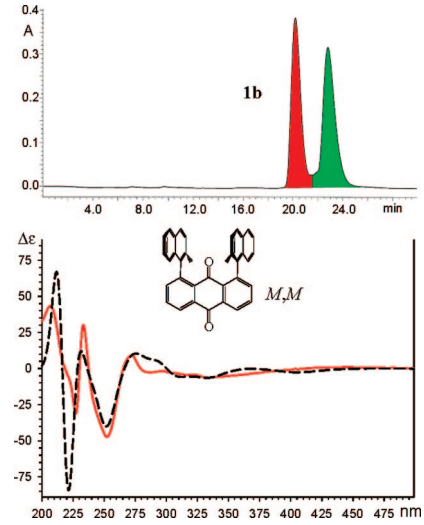

FIGURE 3. (Top) Enantioselective HPLC trace of **1b** (red, first eluted and green, second eluted atropisomer). (Bottom) DFT-computed ECD spectrum for the *M*,*M* configuration (dashed) and experimental spectrum (red) of the first eluted atropisomer.

kcal mol^{-1}. In keeping with this prediction, we were able to separate these derivatives at ambient temperature using HPLC. It is worth noting that the two isolated isomers show different colors, the first eluted being red and the second eluted yellow. This particular behavior is probably due to different interactions between the two naphthalene rings, which are face to face in the *syn* but not in the *anti* isomer.

Structural assignment in solution was unambiguously achieved by ^{1}H NMR spectroscopy, making use of the NOE effect. This approach requires that the ^{13}C satellites of the methyl signal (J_{CH} = 126.3 Hz in both isomers) be simultaneously irradiated.[11,4c]

When applied to the red isomer, this procedure yielded a significant NOE effect at the $^{12}CH_3$ signal, as displayed on the top left side of Figure 1. This proves that this isomer is **1a**, with the *syn* meso structure (C_s point group), because the interproton distance between the two methyl groups (averaged[12] computed value 5.13 Å) is compatible with the detection of a NOE effect. On the contrary, such an effect is not seen in the case of the other (yellow) isomer, which is assigned the *anti* racemic structure **1b** (Figure 1, top right) since in this form the two methyl groups are too far apart (averaged[12] computed distance 7.07 Å).[13]

Single crystals suitable for X-ray diffraction were obtained in the case of *syn*-**1a**, the corresponding structure (Figure 2, bottom) being quite similar to that predicted by DFT calculations (Figure 2, top left). Owing to the slight distortion due to the crystal lattice, however, **1a** does not display, in the solid state, a true C_s symmetry (the dihedral angles between the anthraquinone and naphthalene rings are, in fact, −77.0° and +81.8°).

M,*M* and *P*,*P* enantiomers of the *anti* form **1b** (Scheme 1) were separated by HPLC on a chiral stationary phase, as shown at the top of Figure 3 (the oppositely phased ECD spectra are reported in Figure S-1 of Supporting Information). Comparison of the ECD spectrum computed for the *M*,*M* form (obtained by the TD-DFT method as implemented in the Gaussian program[9]) with that of the first eluted atropisomer, indicated that the latter has the absolute configuration *M*,*M* (Figure 3, bottom traces): the *P*,*P* configuration should be, consequently, assigned to the second eluted. This theoretical approach is quite reliable since it has been convincingly employed several times[14] to predict ECD spectra (in the Supporting Information, the velocity rotational strengths are plotted in Figure S-2, and the transitions energies, oscillator strengths, and rotational strengths of the

(11) Lunazzi, L.; Mazzanti, A. *J. Am. Chem. Soc.* **2004**, *126*, 12155–12157.

(12) The average distances between the methyl hydrogens, used for comparing the NOE effects, were derived from the DFT-computed structures by the relationship $\langle r^{-6}\rangle^{-1/6}$, according to: Claridge, T. D. W. *High-Resolution NMR Techniques in Organic Chemistry*; Pergamon Press: Oxford, 1999; p 303.

(13) This attribution agrees with the trend of the ^{1}H shift of the corresponding methyl groups, that of **1a** (2.02 ppm) being at lower field with respect to that of **1b** (1.68 ppm). The latter should thus correspond to the *anti* structure since its methyl groups lie in a position where they experience the upfield shift displacement due to the aromatic ring currents; see: Jackman, L. M.; Sternhell, S. *Applications of NMR Spectroscopy in Organic Chemistry*, 2nd ed.; Pergamon Press: Oxford, 1969; p 95. Jennings, W. B.; Farrell, B. M.; Malone, J. F *Acc. Chem. Res.* **2001**, *34*, 885–894. Wüthrich, K. *Angew. Chem. Int. Ed.* **2003**, *42*, 3340–3363. Also DFT computations[9] predict an upfield methyl shift for the *anti* (1.71 ppm) with respect to the *syn* (2.16 ppm), in agreement with the observed trend.

(14) For the assignments made by TDDFT-CD calculations, see: Diedrich, C; Grimme, S. *J.Phys. Chem. A* **2003**, *107*, 2524. Stephens, P. J.; McCann, D. M.; Butkus, E.; Stoncius, S.; Cheeseman, J. R.; Frisch, M. J *J. Org. Chem.* **2004**, *69*, 1948. Stephens, P. J.; McCann, D. M.; Devlin, F. J.; Cheeseman, J. R.; Frisch, M. J *J. Am. Chem. Soc.* **2004**, *126*, 7514. Giorgio, E.; Tanaka, K.; Ding, W.; Krishnamurthy, G.; Pitts, K.; Ellestad, G. A.; Rosini, C.; Berova, N. *Bioorg. Med. Chem.* **2005**, *13*, 5072. Stephens, P. J.; McCann, D. M.; Devlin, F. J.; Smith, A. B., III. *J. Nat. Prod.* **2006**, *69*, 1055. Bringmann, G.; Gulder, T.; Reichert, M.; Meyer, F. *Org. Lett.* **2006**, *8*, 1037–1040. Stephens, P. J.; Pan, J.-J.; Devlin, F. J.; Urbanova, M.; Hajicek, J. *J. Org. Chem.* **2007**, *72*, 2508. Casarini, D.; Lunazzi, L.; Mancinelli, M.; Mazzanti, A.; Rosini, C. *J. Org. Chem.* **2007**, *72*, 7667–7676. Goel, A.; Singh, F. V.; Kumar, V.; Reichert, M.; Goulder, T. A. M.; Bringmann, G. *J. Org. Chem.* **2007**, *72*, 7765–7768. Berova, N.; Di Bari, L.; Pescitelli, G. *Chem. Soc. Rev* **2007**, *36*, 914–931.

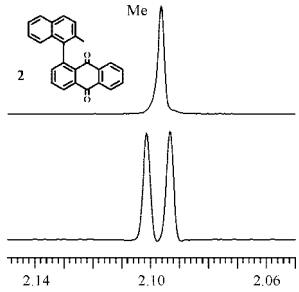

FIGURE 4. Single ^{1}H methyl line (600 MHz in CD_2Cl_2) of **2** (top) splits, at ambient temperature, into two equally intense lines in a chiral environment (bottom).

absolute configuration *M*,*M* for the lowest 90 states are collected in Table S-1 of the Supporting Information).

The kinetics for the *syn*/*anti* interconversion were determined by monitoring the time dependence of the NMR methyl signal of the pure *syn* isomer (**1a**) in a $(CDCl_2)_2$ solution, maintained at +140 °C. The signal of **1a** decreases while that of the *anti* **1b** begins to appear. The intensity of the latter increases until the equilibrium is reached at *anti* (**1b**)/*syn* (**1a**) = 59: 41. This ratio is matched by that (60/40) predicted by DFT calculations at +140 °C.[10] From the first-order kinetics equation for a process at the equilibrium, the appropriate rate constant was obtained (details in Figure S-3 of the Supporting Information). The barrier for exchanging the more stable *anti* (**1b**) into the *syn* (**1a**) was then derived ($\Delta G^{\ddagger}$ = 35.4 kcal mol^{-1} at +140 °C). The mentioned computed value is in acceptable agreement with the experimental result. [15] To check whether the high barrier and the configurational stability of the atropisomers of **1** are dependent on the steric interactions between the two naphthyl groups[16] or whether a single naphthyl substituent is sufficiently large to allow the enantiomer separation, derivative **2** (Chart 1) was also synthesized.

The ambient-temperature ^{1}H NMR methyl signal of **2** (Figure 4) splits into two lines when recorded in the presence of a chiral solvating agent,[17] thus suggesting that the atropisomers of **2** are configurationally stable at ambient temperature. The *P* and *M* antipodes were separated by means of HPLC on a chiral stationary phase and the oppositely phased ECD spectra recorded. Comparison of the computed[14] ECD trace for the *P* form with that of the second eluted atropisomer (Figure S-4 of the Supporting Information) indicates that the latter has the absolute configuration *P*.

The racemization rate constant was determined by following the decreasing proportion of the enantiopure *P* form, kept at +140 °C in a $(CDCl_2)_2$ solution, accompanied by the increasing amount of the *M* atropisomer. The process was monitored by recording the corresponding HPLC signals until the *P* and *M* peaks showed equal intensity, indicating that a complete racemization was achieved (details in Figure S-5 of the Supporting Information). The experimental racemization barrier of **2** ($\Delta G^{\ddagger}$ = 38.0 kcal mol^{-1} at +140 °C) is reasonably reproduced by the computed value (35.6 kcal mol^{-1}) and is close to the interconversion barrier measured in the case of **1**.[15] This indicates that the configurational stability of these atropisomers is essentially due to the steric interaction between a single methylnaphthyl substituent and the carbonyl group of the anthraquinone moiety, rather than to the interaction between the two substituents.

Experimental Section

Materials: 1,8-Bis(2-methylnaphtyl)anthraquinone (1). To a solution of 1,8-dichloroanthraquinone (0.056 g, 0.2 mmol, in 3 mL of benzene) were added K_2CO_3 (2 M solution, 1.0 mL), 2-methylnaphthylboronic acid[18] (0.6 mmol, 0.110 g, suspension in 3 mL of ethanol), and $Pd(PPh_3)_4$ (0.046 g, 0.04 mmol) at room temperature. The stirred solution was refluxed for 2−3 h, the reaction being monitored by GC−MS until the first coupling was complete. After the solution was cooled to room temperature, a second amount of boronic acid (0.6 mmol), K_2CO_3 (2 M solution, 1.0 mL), and $Pd(PPh_3)_4$ (0.046 g, 0.04 mmol) was added and the solution refluxed again for 2−3 h. Subsequently, $CHCl_3$ and H_2O were added, and the extracted organic layer was dried (Na_2SO_4) and evaporated. The crudes were prepurified by chromatography on silica gel (hexane/Et_2O 8:2) to obtain purified mixtures containing the target compounds, and some byproducts as impurities. Pure samples of meso **1a** (red crystals) and racemic **1b** (yellow powder) were obtained by semipreparative HPLC on a C18 column (5 μm, 250 × 10 mm, 5 mL/min, ACN/H_2O 90/10). Single crystals of **1a**, suitable for X-ray diffraction, were obtained by slow evaporation of a chloroform solution.

***anti*-1,8-Bis(2-methylnaphtyl)anthraquinone (1b):** mp 255−257 °C dec; ^{1}H NMR (600 MHz, $CDCl_3$, 25 °C, TMS) δ 1.69 (6H, s), 6.96 (2H, d, J = 8.4 Hz), 7.02 (2H, d, J = 8.5 Hz), 7.18 (2H, t, J = 7.6 Hz), 7.32 (2H, d, J = 7.4 Hz), 7.41 (2H, d, J = 7.6 Hz), 7.53 (2H, d, J = 8.5 Hz), 7.73 (2H, d, J = 8.1 Hz), 7.78 (2H, t, J = 7.6 Hz), 8.43 (2H, d, J = 7.9 Hz); ^{13}C NMR (150.8 MHz, $CDCl_3$, 25 °C, TMS) δ 20.6 (2 CH_3), 124.4 (2 CH), 125.3 (2 CH), 125.7 (2 CH), 126.88 (2 CH), 126.89 (2 CH), 128.0 (2 CH), 128.4 (2 CH), 132.0 (2 q), 132.25 (2 q), 132.26 (2 q), 132.9 (2 CH), 134.4 (2 q), 134.5 (2 q), 136.6 (2 q), 138.5 (2 CH), 140.9 (2 q), 183.1 (C═O), 184.6 (C═O); HRMS(EI) *m*/*z* calcd for $C_{36}H_{24}O_2$ 488.17763, found 488.1779.

***syn*-1,8-Bis(2-methylnaphtyl)anthraquinone (1a):** mp 294−296 °C; ^{1}H NMR (600 MHz, $CDCl_3$, 25 °C, TMS) δ 2.02 (6H, s), 6.82 (2H, d, J = 8.4 Hz), 6.95 (2H, ddd, J = 1.3, 6.7, 8.4 Hz), 7.13 (2H, ddd, J = 1.1, 6.7, 8.4 Hz), 7.17 (2H, d, J = 8.4 Hz), 7.38 (2H, dd, J = 1.3, 7.6 Hz), 7.51 (2H, d, J = 8.3 Hz), 7.55 (2H, d, J = 8.3 Hz), 7.77 (2H, t, J = 7.6 Hz), 8.43 (2H, dd, J = 1.3, 7.6 Hz); ^{13}C NMR (150.8 MHz, $CDCl_3$, 25 °C, TMS) δ 20.6 (2 CH_3), 124.2 (2 CH), 124.7 (2 CH), 125.7 (2 CH), 126.72 (2 CH), 126.74 (2 CH), 127.5 (2 CH), 128.0 (2 CH), 131.51 (2 q), 131.56 (2 q), 131.8 (2 q), 132.7 (2 CH), 133.9 (2 q), 134.3 (2 q), 136.7 (2 q), 138.4 (2 CH), 140.8 (2 q), 182.6 (C═O), 184.4 (C═O); HRMS(EI) *m*/*z* calcd for $C_{36}H_{24}O_2$ 488.17763, found 488.1773.

1-(2-Methylnaphthyl)anthraquinone (2). Compound **2** was prepared using the same procedure described for **1**, using 1-chloroanthraquinone instead of 1,8-dichloroanthraquinone: mp 269−271 dec; ^{1}H NMR (600 MHz, $CDCl_3$, 25 °C, TMS) δ 2.14 (3H, s), 7.11 (1H, d, J = 8.6 Hz), 7.23 (1H, ddd, J = 1.3, 6.7, 8.6 Hz), 7.38 (1H, ddd, J = 1.1, 6.7, 8.0 Hz), 7.47 (1H, d, J = 8.4 Hz), 7.54 (1H, dd, J = 1.4, 7.6 Hz), 7.66 (1H, ddd, J = 1.4, 7.3, 7.6 Hz), 7.73 (1H, ddd, J = 1.4, 7.3, 7.6 Hz), 7.87 (3H, m), 7.97 (1H,

(15) It has to be pointed out that the experimental interconversion is accomplished via the rotation of either of the two naphthalene rings, whereas the computed value was obtained assuming the rotation of only one ring. Thus, for an appropriate comparison the experimental rate constant should be divided by 2 (see, for instance: Lunazzi, L.; Mazzanti, A.; Minzoni, M. *J. Org. Chem.* **2007**, *72*, 2501–2507. Lunazzi, L.; Mazzanti, A.; Rafi, S.; Rao, S.P. *J. Org. Chem.* **2008**, *73*, 678–688). Accordingly, the value of the experimental barrier which actually corresponds to the rotation of a single ring becomes slightly higher, i.e., 35.9 kcal mol^{-1}.

(16) The presence of two substituents might be responsible for the observed interconversion barrier as a consequence of a possible buttressing effect.

(17) A separation of 5 Hz (600 MHz at +25 °C) was observed in a CD_2Cl_2 solution when using a 37:1 molar excess of enantiopure (*R*)-(−)-2,2,2-trifluoro-1-(9-anthryl)ethanol; see: Pirkle, W. H.; Sikkenga, D. L.; Pavlin, M. S. *J. Org. Chem.* **1977**, *42*, 384–387.

(18) Prepared according to: Thompson, W. J.; Gaudino, J. *J. Org. Chem.* **1984**, *49*, 5237.

ddd, J = 0.5, 1.2, 7.8 Hz), 8.30 (1H, ddd, J = 0.5, 1.2, 7.9 Hz), 8.52 (1H, dd, J = 1.4, 7.8 Hz); ^{13}C NMR (150.8 MHz, $CDCl_3$, 25 °C, TMS) δ 20.8 (CH_3), 125.0 (CH), 125.1 (CH), 126.1 (CH), 127.0 (CH), 127.4 (CH), 127.6 (CH), 127.7 (CH), 128.4 (CH), 128.8 (CH), 131.8 (q), 132.1 (q), 132.2 (q), 132.3 (q), 133.2 (q), 133.90 (CH), 133.95 (CH), 134.40 (CH), 134.43 (q), 135.3 (q), 137.9 (q), 138.5 (CH), 142.0 (q), 182.9 (C═O), 183.7 (C═O); HRMS(EI) m/z calcd for $C_{25}H_{16}O_2$ 348.11503, found 348.1151.

HPLC Separation and ECD Spectra. Separation of the two atropisomers of **1b** was achieved at 25 °C using two Chiralcel OD-H 250 × 4.6 mm columns joined together, at a flow rate of 1.0 mL/min, using hexane/*i*-PrOH 98:2 v/v as eluent. UV detection was fixed at 254 nm. Separation of the two atropisomers of **2** was achieved at 25 °C using a Chiralcel AD-H 250 × 20 mm, at a flow rate of 20.0 mL/min, using hexane/*i*-PrOH 90:10 v/v as eluent. UV detection was fixed at 254 nm. UV absorption spectra were recorded at 25 °C in acetonitrile on the racemic mixtures in the 200−500 nm spectral region. The cell path length was 0.1 cm, concentration was 8.2×10^{-5} mol L^{-1} for **1b** and 7.2×10^{-5} mol L^{-1} for **2**. The maximum molar absorption coefficient was recorded at 223 nm for **1b** (ε = 86950) and 226 nm for **2** (ε = 96660). ECD spectra were recorded at 25 °C with the same path lengths of 0.1 cm, in the range 500−200 nm; reported $\Delta\epsilon$ values are expressed as L mol^{-1}cm^{-1}.

Kinetics. Equilibration of the two isomers of **1** was obtained by heating a NMR sample of pure **1a** in $(CDCl_2)_2$ into a thermostatic oil bath, kept at +140 °C. At regular intervals, the sample was taken out from the oil bath and the NMR spectrum recorded at +25 °C until equilibrium was reached. Racemization of the atropisomers of **2** was obtained by heating a sample of enantiopure (*P*)-**2** in $(CDCl_2)_2$ into a thermostatic oil bath, kept at +140 °C. At regular intervals, an aliquot of the sample was taken out from the oil bath, diluted with *i*-PrOH, and analyzed by HPLC on a Chiralcel AD-H column (250 × 4.6 mm, 1.0 mL/min, hexane/*i*-PrOH 90:10 v/v), until the equilibrium was reached.

Calculations. Geometry optimizations were carried out at the B3LYP/6-31G(d) level by means of the Gaussian 03 series of programs[9] (see the Supporting Information): the standard Berny algorithm in redundant internal coordinates and default criteria of convergence were employed. The reported energy values are not ZPE corrected. Harmonic vibrational frequencies were calculated for all the stationary points. For each optimized ground state, the frequency analysis showed the absence of imaginary frequencies, whereas each transition state showed a single imaginary frequency. Visual inspection of the corresponding normal mode was used to confirm that the correct transition state had been found. NMR chemical shift calculations were obtained with the GIAO method at the B3LYP/6-311++G(2d,p)//B3LYP/6-31G(d) level. TMS, calculated at the same level of theory, was used as reference to scale the absolute shielding value. TD-DFT calculations on the *M*,*M* atropisomer of **1b** and the *P* atropisomer of **2** were obtained at the B3LYP/6-31+G(d,p)//B3LYP/6-31G(d) level. In order to cover the whole 500−200 nm range, 90 transitions were calculated in both cases. The CD spectra were then obtained by applying a 0.3 eV Gaussian band shape.[19]

Acknowledgment. L.L. and A.M. received financial support from the University of Bologna (RFO) and from MUR-COFIN 2005, Rome (national project "Stereoselection in Organic Synthesis").

Supporting Information Available: Kinetic data for the **1a**/**1b** equilibration, kinetic data for the racemization of **2**, HPLC separation and ECD spectra of **2**, X-ray data of **1a**, ^{1}H, ^{13}C NMR spectra and HPLC traces of **1** and **2**, and computational data of **1** and **2**. This material is available free of charge via the Internet at http://pubs.acs.org.

JO802383S

(19) (a) GaussSum 2.1.3,2007. Available at http://gausssum.sf.net. (b) O'Boyle, N. M.; Tenderholt, A. L.; Langner, K. M. *J. Comput. Chem.* **2007**, *29*, 839–845.